Jurnal Tribologi 47 (2025) 138-153

MYTRIBOS Malaysian Tribology Society

Jurnal Tribologi

Website : jurnaltribologi.mytribos.org e-issn: 2289-7232

Optimising HTCS-150 die-machined surfaces: Enhancing surface integrity and manufacturing efficiency

Hariz Zuhairi Arif [1], Mohd Hadzley Abu Bakar [2*], Nor Ana Rosli [2], Lailatul Hairina Paijan [2], Mohd Fauzi Mamat [2], Shaiful Anwar Ismail [2], Safarudin Gazali Herawan [3]

[1] Gantract Asia, MALAYSIA.
[2] Faculty of Industrial and Manufacturing Technology and Engineering, Universiti Teknikal Malaysia Melaka, MALAYSIA.
[3] Industrial Engineering Department, Bina Nusantara University, INDONESIA.
*Corresponding author: hadzley@utem.edu.my

KEYWORDS

Die-machined surfaces
HTCS-150
Microscopy
Optimization
Surface integrity

ABSTRACT

High Thermal Conductivity Steel-150 (HTCS-150) has emerged as a specially designed steel that applied in the hot stamping process. Achieving consistent surface quality in hard-to-machine materials like HTCS-150 remains a challenge due to the material's unique thermal and mechanical properties. This study focuses on improving the surface quality of High Thermal Conductivity Steel-150 (HTCS-150) in die machining by controlling milling parameters. Machining trials were done using a carbide ball-end mill with different cutting speeds, feed rates, and depths of cut. Surface roughness was measured, and 3D plots were used to visualize the effects of each parameter. The results showed that depth of cut had the biggest influence on surface finish, followed by feed rate and cutting speed. The best surface roughness achieved was 0.22 µm at 125 m/min cutting speed, 0.30 mm/tooth feed, and 0.1 mm depth of cut. Microscopy confirmed that surface defects like feed marks, smearing, and micro pits appeared when parameters were not applied correctly. This shows that precise control is important to get clean surfaces, especially for stamping die components. The outcome of this study provides practical guidance to improve surface quality and machining efficiency for HTCS-150 applications.

Received 15 July 2025; received in revised form 13 October 2025; accepted 14 October 2025.
To cite this article: Arif et al. (2025). Optimising HTCS-150 die-machined surfaces: Enhancing surface integrity and manufacturing efficiency. Jurnal Tribologi 47, pp.138-153.

1.0 INTRODUCTION

Milling is the operation of removing material with a rotary cutting tool to form the desired shape. During a milling operation, the cutting tool penetrates the workpiece, causing shearing, plastic deformation, chip formation, and forming a new machined surface. Milling operations are commonly used in die machining to produce intricately curved components with a fine surface finish and accurate dimensions. A fine surface finish of stamping dies improves accuracy, surface quality, aesthetics, fatigue strength, and heat-treated ability of the stamped component [1-2].

In milling operation, ball-end mills are commonly used in die machining because they can perform flat or free-form sculptured milling. Ball-end milling reacts differently than flat-end milling because the contact condition is constantly changing. The surface could change from shearing to plowing depending on the contact mechanism, resulting in phenomena such as material side flow, ploughing, or thin chips, which impact the quality, precision, and accuracy of the machined surface [3-5]. Technological advancements have resulted in milling operations making extensive use of the material removal process for stamping dies. For stamping dies, common materials include tool steel up to 62 HRC (AISI D2/SKD 11), cast irons (FC300), tempered steels (AISI D3), and high tempered steels (AISI H13). Specific dies are typically milled from rough to finish conditions and then manually polished to reduce the effect of feed marks. Given that the die is not in the best possible condition after milling, manual polishing is required and takes more time, increasing operational costs and causing muscle fatigue in the operators [6-8].

As an improvement over the familiar cold die steel SKD11, new stamping die steels with high thermal conductivities, such as High Thermal Conductivity Steel-150 (HTCS-150), are being developed. This grade of steel is mainly used for stamping dies to produce high strength steel in the hot stamping process. HTCS-150 is normally equipped with an embedded cooling channel to provide quenching when the sheet metal is stamped inside the die enclosure during the hot stamping process. Machining process for HTCS-150 can be very challenging since this material is expected to have different surface characteristics than conventional dies due to high thermal conductivity of 66 W/m.C. As a result, strategies for machining HTCS-150 with controlled machining parameters are required to assess their impact on surface quality optimisation [9-11].

Because machining stamping dies with ball-end mills requires complicated interaction at the tool-workpiece interfaces, the quantity of work reported on machined surface characteristics has been limited, and the assessment of machining output appears inconsistent. Uhlmann et al. [12] investigated the influence of cutting-edge preparation on the performance of micro milling tools when machining mould steel M261. Their study employed a high-precision three-axis micro milling machine with process monitoring of tool wear, cutting forces, and surface roughness. The results demonstrated that prepared cutting edges, obtained via an immersed tumbling process, significantly improved tool stability by reducing flank wear and crater wear compared to unprepared tools. Although the active forces of prepared and unprepared tools were similar, fluctuations in cutting force decreased with increasing cutting-edge radius, indicating enhanced process stability. Furthermore, the prepared tools achieved better surface quality, with the lowest mean roughness depth (Rz = 0.34 μm) recorded for tools with an edge radius of approximately 4.2 μm. Overall, the findings confirm that cutting edge geometry plays a critical role in tool wear behaviour, force generation, and surface finish, and that micro milling tools with optimised edge preparation exhibit superior performance.

Pan et al. [13] examined the influence of tool orientation—specifically rotational and inclination angles on surface roughness and morphology in ball end milling. Their results showed that surface roughness in the step direction was consistently higher than in the feed direction, and that roughness varied significantly with changes in rotational angle. When the tool orientation was between 30° and 60°, higher cutting speeds at the contact point reduced built-up edge formation and improved surface finish, whereas orientations approaching up-milling conditions increased cold hardening effects and

degraded surface quality. Similarly, the inclination angle strongly affected roughness: both excessively small and excessively large angles resulted in poor surface quality, either due to scraping and squeezing near the tool center at low inclination or due to vibration and tool deflection at high inclination. Surface morphology analyses further confirmed that optimal profiles are difficult to obtain, as the texture and uniformity of the machined surface varied markedly with tool orientation. Collectively, the findings highlight the sensitivity of surface finish to tool axis orientation, underscoring the inherent difficulty in achieving an optimal surface profile in ball end milling.

SEM-based investigations of machined surfaces further confirm the complexity of topographies generated by ball end milling. The study reported in the Bhoplae et al. [14] revealed that the machined surface often exhibits distinct bands, each with different levels of roughness influenced by depth of cut, chip thickness, and tool geometry. Quantitative roughness analysis demonstrated that machining parameters such as cutting speed, feed rate, and depth of cut had their greatest influence in the tool tip zone, where tool wear and incomplete chip removal intensified surface irregularities. Notably, dry machining yielded comparatively lower roughness than chilled air machining, as rapid thermal fluctuations under chilled conditions promoted chipping and surface damage. While higher cutting speeds reduced contact duration and improved finish, the transition between down- and up-milling modes again introduced variability through vibration and chatter. Collectively, these findings emphasize that the inherent geometry of ball end mills produces highly irregular and banded surface morphologies, making surface roughness control particularly challenging near the tool tip where wear effects are most pronounced

This study aims to systematically investigate how key machining parameters such as cutting speed, feed rate, and depth of cut influence the surface quality of High Thermal Conductivity Steel-150 (HTCS-150) in die machining processes. By conducting controlled milling experiments and detailed microscopy analysis, we seek to identify optimal parameter combinations that minimize surface roughness and surface defects such as feed marks and micro pits. The findings will provide practical guidance to enhance manufacturing efficiency and improve the functional performance of stamping dies made from HTCS-150.

2.0 EXPERIMENTAL PROCEDURE

Specific sample of High Thermal Conductivity Steel (HTCS-150) was carefully chosen as the main material for this study. The sample was cut precisely to 70 mm by 70 mm. This material is well-known for strong mechanical and thermal properties. The combination of Mo and Mn helps increase toughness, resistance to torsion, and fatigue strength. At the same time, the presence of Cu contributes to better thermal conductivity. Each sample, already hardened up to 52 HRC, went through a proper cleaning and light skimming process to make sure the surface was flat and smooth. Such preparation was important to ensure the machining trials could produce accurate and reliable results. The specific characteristics of HTCS-150 are listed in Table 1.

Machining trials on HTCS-150 started with the use of an SFRT20 carbide ball-end mill, as shown in Figure 2. This tool, attached to an SRFH20S02L80 tool holder, was operated using the DMU 60 CNC milling machine, as illustrated in Figure 2(a-b). The selected parameters which are cutting speed (Vc), feed rate (Fz), and depth of cut (ap) were set based on references from industry practices, where the same workpiece material and cutting tools were used. Preliminary trials were carried out to identify parameter ranges that could safely avoid tool damage and specimen deformation while enabling measurable variation in surface roughness. A review of prior studies involving similar hard-to-machine materials, such as tool steels and stamping dies, informed the selection of parameter levels to ensure comparability of results. Additionally, the chosen ranges (cutting speed: 120 to 130 m/min, feed rate: 0.3 to 0.5 mm/tooth, depth of cut: 0.1 to 0.5 mm) reflect real-world machining conditions

typically applied in industry settings for HTCS-150 or comparable alloys. These values provide a comprehensive yet practical exploration of the machining parameter space to optimize surface quality.

To handle the complexity of the milling process, the Box-Behnken experimental design was used together with Response Surface Methodology (RSM), which is detailed in Table 2. Once the cutting length reached 50,000 mm, surface roughness was measured carefully using a Mitutoyo Surface Roughness Tester, shown in Figure 2(c). To further analyse the surface condition, the machined HTCS-150 was observed under a Scanning Electron Microscope, providing a clear view of the surface profile and revealing the detailed effects of the machining process.

Table 1: Properties of HTCS-150 steel.

Properties	**Conditions**
Surface Roughness (as received)	0.45 µm
Hardness	52 Hrc
Density	7.97 x 10^3 Kg/m^3
Mechanical Strength	1305 Mpa
Yield Strength	1233 Mpa
Density (kg/m^3)	7970
Elastic Modulus (GPa)	216
Yield Strength at 25^{o}C-450^{o}C (MPa)	858-1233
Thermal Conductivity (W/m.C)	66
Heat Capacity (J/kg.C)	496

Figure 1: The cutting tool used in this study resembles the SFRT20 specification.

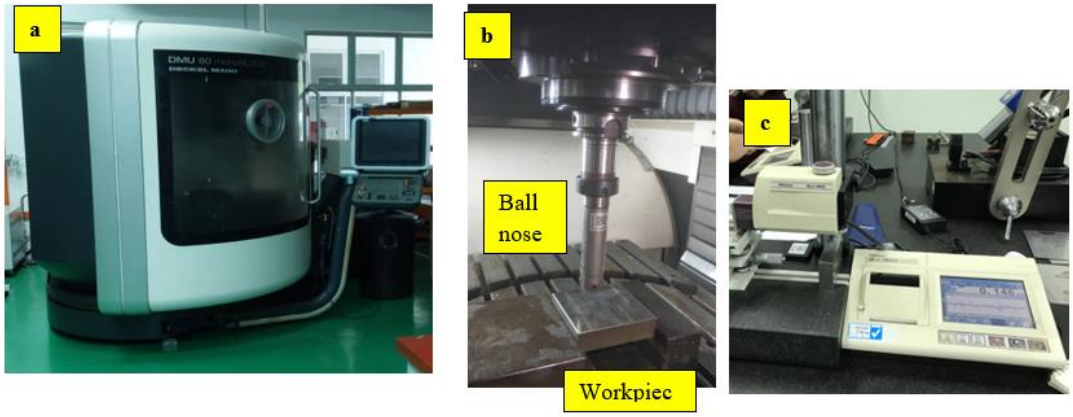

Figure 2: (a) CNC milling machine (DMU 60 Monoblock); (b) Machining setup; (c) Mitutoyo surface roughness tester.

Table 2: Design of experiment for the machining trials.

Std Run	Machining Parameters			Average Surface Roughness (μm)
	Cutting Speed, V_c (m/min)	Feed Rate, F_z (mm/tooth)	Depth of cut, a_p (mm)	
1	120	0.3	0.3	0.450
2	130	0.3	0.3	0.344
3	120	0.5	0.3	0.412
4	130	0.5	0.3	0.720
5	120	0.4	0.1	0.300
6	130	0.4	0.1	0.390
7	120	0.4	0.5	0.506
8	130	0.4	0.5	0.630
9	125	0.3	0.1	0.220
10	125	0.5	0.1	0.430
11	125	0.3	0.5	0.470
12	125	0.5	0.5	0.560
13	125	0.4	0.3	0.256
14	125	0.4	0.3	0.360
15	125	0.4	0.3	0.280
16	125	0.4	0.3	0.351
17	125	0.4	0.3	0.276

3.0 RESULTS AND DISCUSSION

To statistically evaluate the effects of cutting speed, feed rate, and depth of cut on surface roughness, Analysis of Variance (ANOVA) was performed. The results, summarized in Table 3, indicate that all three parameters significantly influence surface finish, with depth of cut showing the greatest impact ($p < 0.01$). The interaction effects between feed rate and depth of cut were also statistically significant, suggesting that these factors jointly affect the machining outcome. The coefficient of determination (R^2) for the model was calculated as 0.9548, indicating a good fit with 95% of the variability in surface roughness explained by the model. These statistical measures confirm the robustness of the Response Surface Methodology and substantiate the significance of machining parameters in optimizing the surface finish of HTCS-150 dies [9-10]. The model, which includes factors A, B, C, AB, A^2, B^2, and C^2, is shown in equation (1).

Surface Roughness (μm) =+76.79312 - 1.13940 (Cutting Speed) -30.69350 (Feed rate) -0.161750 (axial depth of cut) + 0.207000 (Cutting Speed. Feed rate) + 0.00426 (Cutting Speed)^2 + 7.02000 (Feed rate)^2 +1.13000 (axial depth of cut) ^{2} (1)

Table 3: ANOVA analysis table for surface roughness response.

Source	Sum of Squares	Df	Mean Square	F-Value	p-Value	
Model	0.2857	7	0.0408	26.93	< 0.0001	Significant
A (cutting speed)	0.0216	1	0.0216	14.27	0.0044	
B (feed rate)	0.0509	1	0.0509	33.57	0.0003	
C (depth of cut)	0.0853	1	0.0853	56.28	< 0.0001	
AB	0.0428	1	0.0428	28.27	0.0005	
A^2	0.0479	1	0.0479	31.63	0.0003	
B^2	0.0207	1	0.0207	13.69	0.0049	
C^2	0.0086	1	0.0086	5.68	0.0411	
Residual	0.0136	9	0.0015			
Lack of Fit	0.0046	5	0.0009	0.4114	0.8218	not significant
Cor Total	0.2993	16				
R^2	0.9548	(0.2857/0.2993)				

The validation of all data through ANOVA has been carried out in [10], where the average difference between experimental values and ANOVA results is approximately 5.25%. This indicates that the accuracy level is within 10%, confirming that the model is highly reliable. Therefore, the model is suitable for predicting subsequent machining parameters.

Figure 3 and Figure 4 present the 3D plot outcomes derived from Table 2, with the selected constant depths of cut at 0.2 mm and 0.5 mm, respectively. These 3D plots offer a clearer understanding of how machining parameters, particularly surface roughness, cutting speed, and feed rate, interact during the milling process. The narrow window of ideal conditions shows that the process is highly sensitive, where even small deviations can significantly impact the surface finish. A smoother and more consistent surface is achieved when the interaction between the tool and the material is properly balanced.

These visual representations emphasise the importance of precise control to achieve a good surface finish. From the plots, a clear relationship can be observed between cutting speed and feed rate, especially under different depths of cut. The data highlights that both parameters must be carefully balanced to ensure consistent and high-quality machining results. Maintaining this level of control is essential in producing fine machined surfaces. This insight is useful when selecting suitable parameters, especially for applications where surface quality is a critical requirement [14–16].

Figure 3, for example, shows how surface roughness changes when cutting speed and feed rate are adjusted, while keeping the depth of cut constant at 0.2 mm. The smoothest surface was recorded when the cutting speed ranged from 126 to 127 m/min, with a feed rate close to 0.31 mm/tooth. When the depth of cut increased to 0.5 mm, as shown in Figure 4, the optimal cutting speed stayed roughly the same. However, the acceptable feed rate range became wider, between 0.3 and 0.4 mm/tooth. Although depth of cut is the most significant factor, there are situations where slight adjustments to the feed rate allow some flexibility in the effect of depth of cut. However, this does not reduce its influence as the dominant parameter. This suggests that the process allows a bit more flexibility, which is useful in real machining situations where slight variations in parameters may occur. Even with those changes, surface roughness remained low.

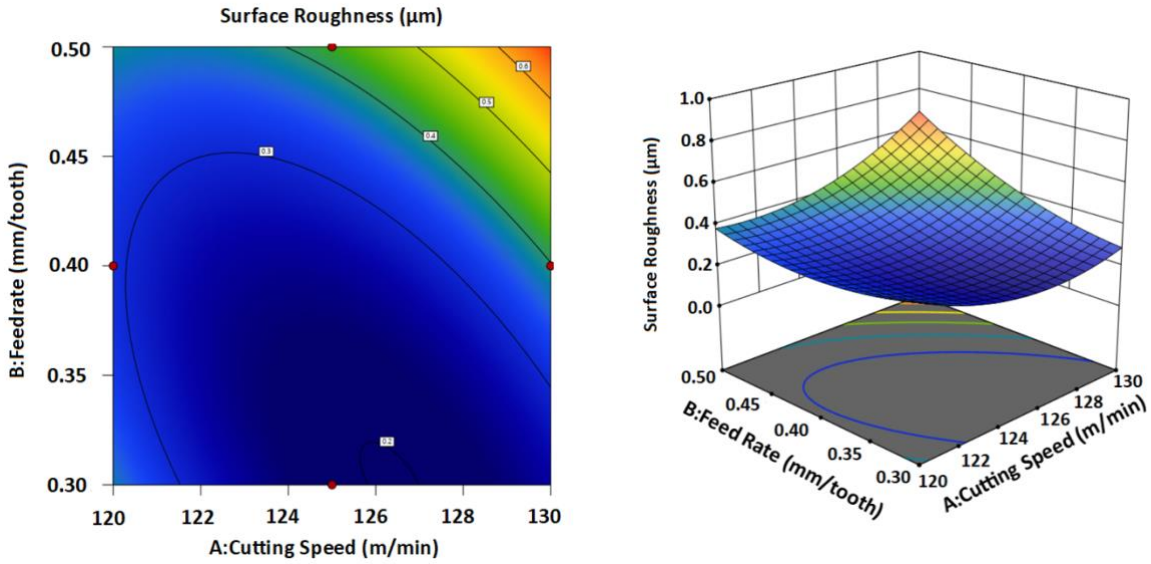

Figure 3: Effect of feed rate and cutting speed on surface roughness at a constant depth of cut of 0.2 mm.

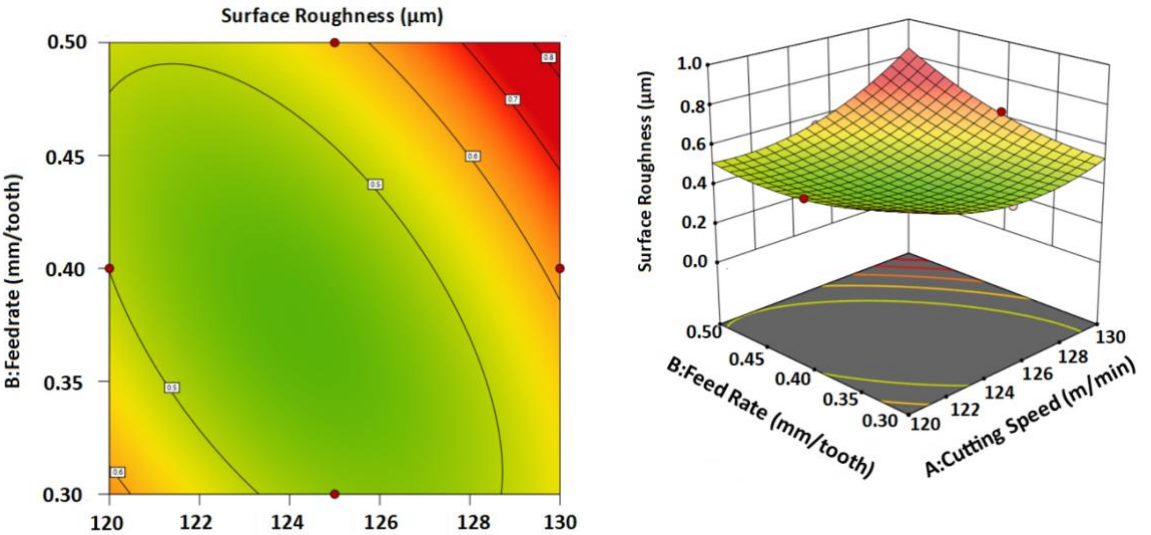

Figure 4: Effect of feed rate and cutting speed on surface roughness at a constant depth of cut of 0.5 mm.

For both graphs, the consistent results seen at cutting speeds around 125 to 127 m/min indicate a good balance point. This may be because of controlled heat generation, less tool wear, and efficient chip removal. Operating within this range is very important, especially when surface finish is a critical requirement. This trend is quite similar to the findings from Sheikh et al. [15]. In their research, surface finish improved with increasing cutting speed, up to a certain level. After that, the quality started to decline. They also pointed out that using a lower feed rate can help

achieve a smoother surface, as long as it is paired with the right cutting speed. These findings closely match what has been observed in this current study.

Table 4 compares our optimized machining parameters and surface roughness values with those reported in key literature. For instance, Scandiffio et al. [16] reported a minimum surface roughness of 0.15 μm, finer than the 0.22 μm obtained in this study, as their cutting speed was set at 360 m/min, whereas a lower speed was applied here. Differences observed with Magalhaes et al. [17] may stem from varying region and type of milling whether climb or down, illustrating the importance of process parameter optimization tailored to specific contexts. Our lower roughness values indicate that precise control of feed rate and cutting depth, in addition to cutting speed, plays a critical role in improving surface integrity. Mali et al. [18] demonstrated that a balanced combination of process parameters, region and cutting path strategies helps optimize both surface quality and tool life, with surface roughness ranging between 0.390 and 0.842 μm. Our findings corroborate this and extend the understanding to the specific context of HTCS-150 die machining. Together, these comparisons underscore the practical significance of our optimized parameters and support their adoption for improving manufacturing efficiency and product durability in industrial applications involving HTCS-150.

Considering the die's properties are consistent, it is expected that optimal machining performance can be achieved based on the parameters from the 3D plot. However, the results may not be consistent if certain areas of the die possess different characteristics, leading to variations in machining outcomes. Figures 5 and 6 showcase various qualities of the machined surfaces. Figure 5 presents surfaces with fine finishes, ranging from 0.220 μm to 0.450 μm in surface roughness. In Figure 5(a), the surface from standard run 9 displays a smooth and bright finish with a roughness of 0.220 μm, indicating an effective combination of cutting parameters that ensured a clean cut. Figure 5(b) illustrates a surface from standard run 17 with uniform flatness and a regular scalloped texture, indicative of well-controlled machining conditions. Conversely, Figure 5(c) reveals a surface with a roughness of 0.450 μm, showing defects likely due to the casting process of the workpiece, though the surface remains relatively clean.

Figure 6, on the other hand, depicts surfaces with rough finishes, ranging from 0.470 μm to 0.720 μm. Figure 6(a) shows a surface from standard run 11 with a roughness of 0.470 μm, exhibiting uneven ploughing and irregular smeared material. Figure 6(b) presents a deteriorated surface from standard run 17, characterized by uneven shearing and material fragments. Finally, Figure 6(c) highlights significant surface defects from standard run 1, including macro-cracks and anisotropic feed marks, resulting from the rotational cutting tool's shearing action and insufficient overlap rate.

Table 4: Comparative table of machining parameters and surface roughness.

Study	**Material**	**Cutting Speed (m/ min)**	**Feed Rate (mm/ tooth)**	**Depth of Cut (mm)**	**Surface Rough-ness (µm)**	**Notes**
Current Study	HTCS-150	120-130	0.3	0.1	0.22	Optimized parameters, lowest roughness, constant tool-path, flat surface
Scandiffio et al. [16]	AISI D2 (60 HRC)	360	0.1	0.2	0.15-0.56	Higher roughness is caused by tool path and cutting region
Magalhaes et al. [17]	Hardened AISI H13	150	0.033	0.25	1.5-5.0	Tool-path strategy plays an important role in achieving low surface roughnes
Mali et al. [18]	Aluminum alloy	47-141	0.05-0,15	0.2-0.6	0.20-4.40	The variation in surface roughness depends on the chosen tool-path strategy and the cutting region

(a) Std run : 2 (130 m/min, 0.3 mm/tooth, 0.3 mm) Surface roughness: 0.256 µm	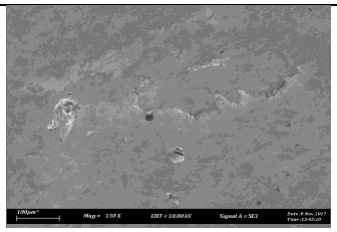
(b) Std run : 3 (120 m/min, 0.5 mm/tooth, 0.3 mm) Surface roughness: 0.412 µm	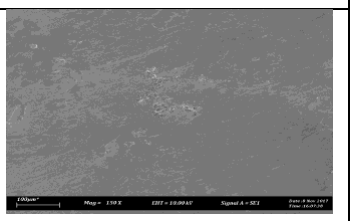
(c) Std run : 13 (125 m/min, 0.4 mm/tooth, 0.3 mm) Surface roughness: 0.256 µm	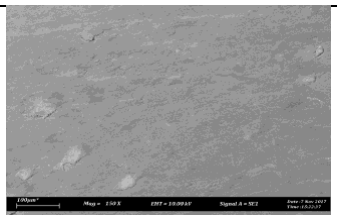

Figure 5: Surface roughness ranged from 0.256 µm to 0.412 µm, indicating fine surface finishes.

a) Std run : 7 (120 m/min, 0.4 mm/tooth, 0.5 mm) Surface roughness: 0.506 μm	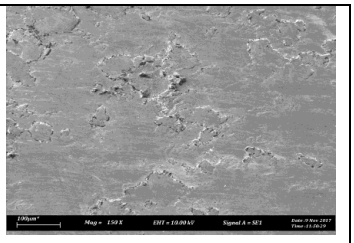
b) Std run : 8 (130 m/min, 0.4 mm/tooth, 0.5 mm) Surface roughness: 0.630 μm	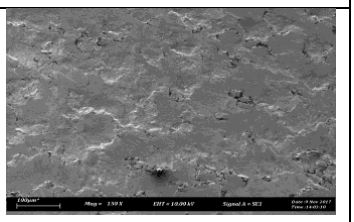
c) Std run : 12 (125 m/min, 0.5 mm/tooth, 0. mm) Surface roughness: 0.560 μm	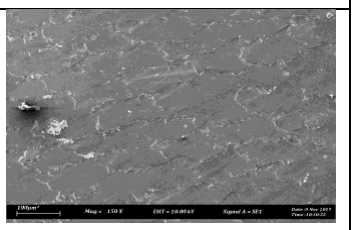

Figure 6: Surface roughness ranged from 0.506 μm to 0.630 μm, indicating relatively coarse finishes.

Figures 7-11 show additional observations of machined surface profiles at the microscopy level. The first surface profile observation that should be emphasized is the formation of feed marks along the machined surface. This is shown in Figure 7, where the workpiece surface at standard run 6 clearly exhibits scratch of feed marks approximately 50 μm. It was suggested that the small grit of chips that slide along the cutting path responsible for the inherent scratching. Small grit chips produced during machining could become trapped at the tool-workpiece interfaces after becoming displaced from the workpiece. Such trapped grits may scratch the surface of the machined component, leaving an inherent feed mark along the cutting path [19-21].

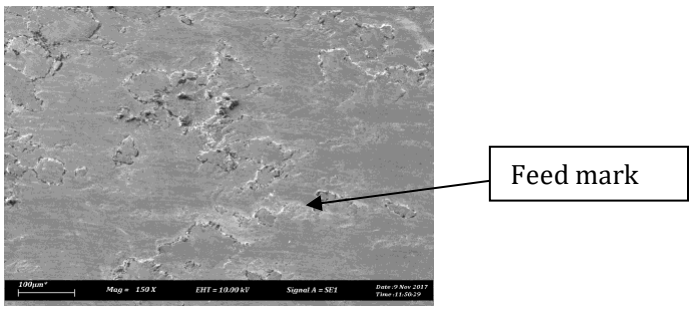

Figure 7: Feed mark on workpiece surface observed at standard run 7 (120 m/min cutting speed, 0.4 mm/tooth feed rate and 0.5 mm depth of cut).

The second characteristic of the surface profile that can be emphasized is the development of smeared materials along the cutting path. Figure 8 shows the observation on the machined surface where smeared material was visible in the form of adherent particles. Material smearing occurred due to the high cutting heat generated during machining surpassed the thermal stability limit and induced plasticity of the workpiece. Partial of the softened workpiece is readily to be shattered as the cutting tool shears the material. To some extent, the workpiece material's softening state could also lead to separation from the cutting zone and reattach on the machined surface [20-22]. The surface roughness will then increase if there have been several smearings at the machined surface.

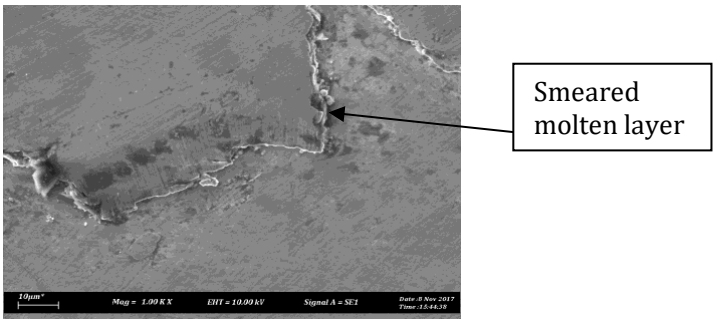

Figure 8: Smeared molten layer was observed on the workpiece surface during standard run 2 (cutting speed: 120 m/min, feed rate: 0.30 mm/tooth, depth of cut: 0.30 mm).

Another observation on the machined surface that must be addressed is the appearance of micro-pits or porosity along the cutting path. Figure 9 shows the presence of these characteristics as small dark spots. The porosity observed in Figure 9 is expected to originate primarily from material preparation rather than the milling process. HTCS-150 is produced through a casting route, and a certain degree of micro-porosity may result from air entrapment or inclusions during solidification. However, during milling, these existing voids may become more visible or slightly enlarged due to material removal from tool interaction.

To some extent, the appearance of porosity can also develop when particles from the workpiece detach due to the inherent sliding of the tool's nose radius at the contact interface. Such small detachments create voids within the workpiece structure, potentially causing stress concentration or disrupting tool–workpiece engagement during machining. The number of pores may increase if cutting conditions are not carefully controlled. The development of porosity increases the risk of fatigue failure in the stamping die [23–24].

Zhang et al. (2024) investigated the effects of air entrapment on the mechanical properties of magnesium alloy castings, finding that air pockets formed during the casting process could lead to porosity. This porosity weakened the overall strength and ductility of the material, highlighting the critical role of proper mold design and controlled pouring techniques in minimizing air entrapment and ensuring casting quality. This aligns with the current findings, where inconsistencies during manufacturing likely resulted in similar porosity and defects on the surface, further underscoring the importance of controlled manufacturing processes [28-29].

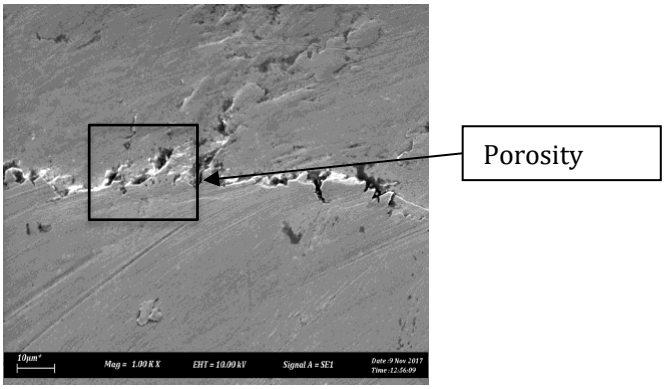

Figure 9: Porosity on the workpiece surface observed at standard run 10 (125 m/min cutting speed, 0.50 mm/tooth feed rate and 0.10 mm depth of cut)

Observations across some other machined surfaces reveal surface irregularities, particularly in areas that seem imperfection, as shown in Figure 10 and Figure 11. This surface irregularities may be due to inconsistencies during the manufacturing process, possibly involving the introduction of particles with varying hardness levels, resulting in non-uniform solidification. Although these surface irregularities appear to be isolated, they are prevalent across the surface, potentially leading to recurring issues during repeated operations. Such surface defects could significantly impact the component's performance and longevity [25-28].

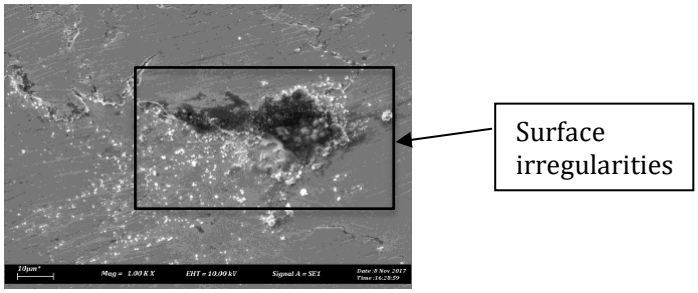

Figure 10: Surface irregularity on the workpiece surface observed at standard run 16 (125 m/min, 0.4 mm/tooth, 0.3 mm).

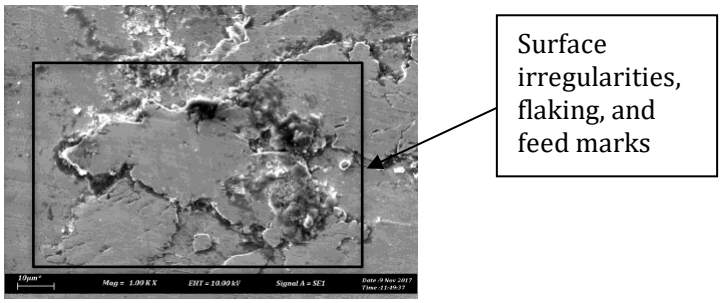

Figure 11: Surface irregularities, flaking, and feed marks observed at standard run 7 (120 m/min, 0.4 mm/tooth, 0.5 mm depth of cut).

In this study, the optimized parameters have the potential to yield commercial benefits in terms of cost reduction and improved manufacturing efficiency for HTCS-150 steel specifications. For example, the optimized milling parameters (125 m/min cutting speed, 0.30 mm/tooth feed, 0.1 mm depth of cut) produce a superior surface finish (average roughness 0.22 μm), that produce a good surface finish can reduce the need for secondary operations such as intensive manual polishing. Based on current polishing times and labor costs, this could reduce polishing time by approximately 20%. For instance, if manual polishing currently takes 2 hours per die at an operator cost of RM20 per hour, the cost saving per die can be calculated using equations (2) and (3)[29-30].

Time saved = 2×0.20=0.4 hours (2)
Cost saved = 0.4×20=RM8 per die (3)

Among the key benefits that can be interpreted from this study is the reduction in cutting tool costs per die production. By selecting appropriate cutting speeds and feed rates, tool wear can be minimized. A tool life improvement of up to 20% can be achieved when machining is performed under optimized conditions.

Assuming a tool replacement cost of RM200 and an average tool life of 20 dies, the cost per die under normal conditions is RM10. With a 20% improvement in tool life, the number of dies produced per tool increases to 24, reducing the cost per die to approximately RM8.33. This translates to a savings of RM1.67 per die.

In addition, by minimizing rework operations for each die, it can also reduce and save operational costs in terms of rework tasks as well as repolishing or regrinding processes. Assuming that each operation can reduce approximately 5% of total defects, the effective increase in yield will result in a reduction in labor costs for each die. For example, the cost savings from reduced rework of 100 HTCS-150 dies valued at RM100 each can be calculated using equation (4).

5%×RM100=RM500 per 100 dies (4)

Overall, this optimization has the potential to generate savings for each die produced through improved manpower efficiency, tool usage, and other direct benefits. In large-scale production, these savings can translate into significant cost reductions and enhanced competitiveness [31-32].

CONCLUSIONS

(a) The results have shown that machining parameters play a key role in determining surface integrity for HTCS-150 steel. Based on the statistical model and 3D surface plots from RSM analysis, the optimum machining parameters for achieving the lowest surface roughness (Ra = 0.22 μm) in HTCS-150 were determined as follows:
    - Cutting speed (Vc): 125 m/min
    - Feed rate (Fz): 0.30 mm/tooth
    - Depth of cut (ap): 0.10 mm

These parameters represent the best trade-off between machining stability, surface finish, and tool life. The optimized condition also minimizes secondary finishing processes and enhances die surface integrity.

(b) Surface inspection confirmed that these settings produced fine finishes. When parameters moved outside this range, defects such as ploughing, smeared areas, and micro-cracks started to appear. This supports the importance of using optimised machining conditions.

(c) Microscopic surface analysis highlighted how important it is to maintain accurate control over parameters. Defects like feed marks and porosities not only affect appearance but can also increase the risk of fatigue failure.

(d) The use of optimized machining parameters has the potential to reduce polishing, regrinding, or rework time by up to 20%. It is expected to extend the service life of cutting tools by approximately 20% improved surface finish. Consequently, this can enhance production output, reduce labor costs, and lower tooling expenses. Ultimately, it increases overall efficiency while demonstrating strong commercial potential in the production of HTCS-150 dies.

(e) Future research should consider factors such as coolant use and tool material. Long-term die performance studies would clarify durability, while advanced methods such as X-Ray or thermography could reveal finer surface details. Industrial testing is also essential to validate applicability in production, along with tool wear and life-cycle analysis under real stamping conditions.

(f) The outcome from this study has good commercial potential. Industries that rely on high-quality die surfaces could benefit through better machining efficiency, fewer defects, and lower maintenance costs. These findings can also be applied to other materials and processes across multiple sectors.

ACKNOWLEDGEMENT

The authors gratefully acknowledge the support provided by Universiti Teknikal Malaysia Melaka (UTeM) for financial assistance under FRGS/1/2024/FTKIP/F00569.

REFERENCES

[1] Astakhov, V. P., Petropoulos, G. P., Pandazaras, C. N., & Davim, J. P. (2024). Surface integrity – Definition and importance in functional performance. In Surface Integrity in Machining (pp. 1–35). Springer.

[2] Brown, A., & Wilson, P. (2024). Parametric optimization in precision machining. Precision Engineering, 78, 234–245.

[3] Chen, L., Zhang, Y., & Liu, H. (2024). Advances in surface integrity of machined components. International Journal of Machine Tools and Manufacture, 98, 45–58.

[4] Davis, R., & Lee, S. (2023). Advances in SEM and AFM for surface characterization. Journal of Microscopy, 280(3), 215–228.

[5] Kim, S., Park, J., & Lee, D. (2023). Surface defects in die machining: Causes and solutions. Journal of Materials Processing Technology, 295, 117–125.

[6] Grum, J. (2024). Residual stresses and microstructural modifications. In Surface Integrity in Machining (pp. 67–126). Springer.

[7] Li, X., & Zhang, Y. (2021). Challenges in machining high-performance steel alloys. Materials Science and Engineering A, 812, 141–150.
[8] Jackson, M. J. (2024). Surface integrity of micro and nanomachined surfaces. In Surface Integrity in Machining (pp. 181–211). Springer.
[9] Hadzley, A., Azahar, W., Anis, A., Izamshah, R., Amran, M., Kasim, S., & Noorazizi, S. (2019). Development of surface roughness prediction model using response surface methodology for end milling of HTCS-150. Journal of Advanced Manufacturing Technology (JAMT), 12(1), 467–476.
[10] Mohd Rashid, M. F., Abu Bakar, M. H., Mamat, M. F., Paijan, L. H., Rosli, N. A., Ab Wahab, N., & Herawan, S. G. (2024). Optimization of cutting parameters for surface roughness and microscopy analysis in machining hardened high thermal conductivity 150 (HTCS-150) steel. Malaysian Journal of Microscopy, 20(2), 133-144.
[11] Yang, F., & Chen, Z. (2023). Thermal conductivity and hardness challenges in machining HTCS-150 steel. Journal of Materials Research, 38(4), 567–578.
[12] Uhlmann, E., Oberschmidt, D., Löwenstein, A., & Kuche, Y. (2016). Influence of cutting edge preparation on the performance of micro milling tools. Procedia CIRP, 46, 214–217.
[13] Pan, Y., Changfeng, Y., Shaohua, X., Dinghua, Z., & Xingtang, D. (2016). Effect of tool orientation on surface integrity during ball end milling of titanium alloy TC17. Procedia CIRP, 56, 143–148.
[14] Bhopale, N. N., & Pawade, R. S. (2015). Effect of ball end milling parameters on surface and subsurface of Inconel-718. International Journal of Basic and Applied Sciences, 4(1), 66–72.
[15] Sheikh, A. H., Mandal, B. B., Sarkar, A., Baig, M., Alharthi, N., & Alzahrani, B. (2019). Application of response surface methodology for prediction and modeling of surface roughness in ball end milling of OFHC copper. International Journal of Mechanical and Materials Engineering, 14(1), 3
[16] Scandiffio, I.; Diniz, A.E.; de Souza, A.F.; Evaluating surface roughness, tool life, and machining force when milling free-form shapes on hardened AISI D6 steel Int. J. Adv. Manuf. Technol. 2016, 82, 2075–2086.
[17] Magalhães, L. C., & Ferreira, J. C. E. (2019). Assessment of tool path strategies for milling complex surfaces in hardened H13 steel. Proceedings of the Institution of Mechanical Engineers, Part B: Journal of Engineering Manufacture, 233(5), 834–849
[18] Mali, R. A., Aiswaresh, R., & Gupta, T. V. K. (2020). The influence of tool-path strategies and cutting parameters on cutting forces, tool wear and surface quality in finish milling of Aluminium 7075 curved surface. The International Journal of Advanced Manufacturing Technology. Advance online publication.
[19] Smith, J., & Brown, T. (2024). 3D plotting for visualizing machining parameters. Journal of Manufacturing Systems, 62, 89–101.
[20] Zhang, H., & Li, M. (2023). Microscopy techniques for surface analysis in die machining. Microscopy and Microanalysis, 29(2), 345–356.
[21] Zhou, Y., Li, X., & Wang, J. (2024). Surface integrity in die machining: A comprehensive review. Journal of Materials Processing Technology.
[22] Prado, M. T., Pereira, A., Pérez, J. A., & Mathia, T. G. (2017). Methodology for tool wear analysis by a simple procedure during milling of AISI H13 and its impact on surface morphology. Procedia Manufacturing, 13, 348–355.

[23] Thamizhmanii, S., Yuvaraj, C., Senthilkumara, J. S., & Sulaiman, A. I. (2019). Effect of feed rate on difficult-to-cut metals on surface roughness and tool wear using surface treated and untreated tools. Procedia Manufacturing, 30, 216–223.
[24] Komatsu, W., & Nakamoto, K. (2021). Machining process analysis for machine tool selection based on form-shaping motions. Precision Engineering, 67, 199–211.
[25] Salem, A., Hega, H., & Kishawy, H. A. (2021). An integrated approach for sustainable machining processes: Assessment, performance analysis, and optimization. Sustainable Production and Consumption, 25, 450–470.
[26] Kim, S., Park, J., & Lee, D. (2023). Surface defects in die machining: Causes and solutions. Journal of Materials Processing Technology, 295, 117–125.
[27] Ghosh, G. K., & Banerjee, A. K. (2023). Effects of casting conditions on surface defects of castings. Journal of Materials Processing Technology, 295, 117–125.
[28] Pimenov, D. Y., Kiran, M., Khanna, N., Pintaude, G., Vasco, M. C., & da Silva, L. R. R. (2023). Review of improvement of machinability and surface integrity in machining on aluminum alloys. The International Journal of Advanced Manufacturing Technology, 129, 4743–4779.
[29] Zhang, Y., Liu, R., & Wang, C. (2024). Recent progress on cast magnesium alloy and components. Journal of Materials Science, 59, 9969–10002.
[30] Shane. (2025, June 22). How to calculate and optimize die casting costs. MFG Shop. https://shop.machinemfg.com/die-casting-cost-how-to-calculate-and-optimize/
[31] Bendul, J., & Apostu, V. (2017). An accuracy investigation of product cost estimation in automotive die manufacturing. International Journal of Business Administration, 8(7), 1–12.
[32] Rozeman, S., Adesta, E. Y. T., Sophian, A., & Tomadi, S. H. (2023). Improvement activities in stamping die manufacturing: A systematic literature review. International Journal of Engineering Materials and Manufacture, 8(2), 21–35